Journal of Alloys and Compounds 501 (2010) 375–379

Contents lists available at ScienceDirect

Journal of Alloys and Compounds

journal homepage: www.elsevier.com/locate/jallcom

Aqueous phase approach to ZnO microspindles at low temperature

Lihong Gong [a,b], Xiang Wu [b,*], Cai Ye [b], Fengyu Qu [b], Maozhong An [a,*]

[a] *College of Chemical Engineering and Technology, Harbin Institute of Technology, Harbin 150001, PR China*
[b] *College of Chemistry and Chemical Engineering, Harbin Normal University, Harbin 150025, PR China*

ARTICLE INFO

Article history:
Received 5 February 2010
Received in revised form 13 April 2010
Accepted 14 April 2010
Available online 22 April 2010

Keywords:
Semiconductor
ZnO
Microcrystals
Optical property

ABSTRACT

ZnO microspindles with average diameter of 200 nm and length of about 1 μm have been successfully synthesized via a simple solution route at low temperature. The morphologies, crystal structure, chemical compositions of the products are characterized by scanning electron microscopy, X-ray powder diffraction, transmission electron microscopy and Raman spectroscopy. It was found that the as-synthesized ZnO microspindles are single crystals with wurtzite structure and with the preferred [0 0 0 1] growth direction. A strong visible emission centered at 423 nm and a weak emission at 484 nm were observed, which may be due to the defects associated to the structures. ZnO microspindles prepared here may find potential applications in electronic and optoelectronic fields.

1. Introduction

Over the past few years, much attention has been paid to the synthesis of one-dimensional (1D) semiconductor nanomaterials with controlled structures, shapes, and compositions owning to their special properties and potential applications in various fields, such as being used to fabricate nanoscale devices, including sensors [1], field emitters [2,3], light-emitting diodes [4], vacuum gauges [5], nanofloating gate memories [6], solar energy cells [7], piezo-nanogenerators [8] and so on. The observed 1D nanostructures include nanowires [9], nanorods [10,11], nanorings [12], nanochains [13], nanohelix [14], and fishbone-like nanostructures [15], etc. And several methods have been demonstrated to prepare 1D nanostructures, including metal-organic chemical vapor deposition (MOCVD) [16], molecular beam epitaxy (MBE) [17], thermal evaporation [18–20], hydrothermal method [21,22], and template-based growth [23,24]. Although many research efforts have been directly paid to synthesize oriented 1D semiconductor nanomaterials, it still remains challenging to synthesize 1D nanostructures with special morphologies, such as spindle-like structure, on large scale, which is important to realize the fabrication and integration of nanoscale devices for scientific and technological applications.

ZnO is an important direct band-gap semiconductor with a band gap of 3.37 eV and large exciton binding energy of 60 meV. It has important applications in optics and optoelectronics fields. So far, diversiform morphologies of ZnO nanostructures have been synthesized via different methods. Among them, the solution method appears as a very powerful method and has been widely used to grow ZnO nanostructures. Solution method does not involve complex procedures, sophisticated equipment, or rigid experimental conditions. In this paper, utilizing a simple solution method, we successfully synthesized spindle-like ZnO microcrystals without using any surfactant or template at a low temperature of 75 °C. Morphologies, structures and optical property of as-synthesized products are investigated via different techniques and the effects of experimental parameters on the morphologies are also investigated.

2. Experimental

All reagents are analytical grade and were used without further purification. A typical experimental procedure is described as follows: 0.002 M zinc nitrate ($Zn(NO_3)_2$) was dissolved into 25 ml distilled water in a 50 ml glass beaker with stirring until the solution was transparent. Then 5 M sodium hydroxide was added dropwise into the above solution under ceaselessly magnetic stirring until the pH value of the solution reached 10. The solution was then maintained at 75 °C for about 11 h under constant stirring. After that, the solution was cooled to room temperature in the still state. Then the resulting products were collected, washed several times with de-ionized water and alcohol in sequence, and then dried at 60 °C for 12 h. The white product was finally annealed in an oven at 600 °C for 2 h. The compared experiments were carried out following the same procedure.

The samples were characterized with scanning electron microscopy (SEM, Hitachi-4800), transmission electron microscope (TEM, JEOL 2010EX) with energy dispersive X-ray spectrum (EDS), X-ray powder diffraction (XRD, Rigaku Dmax-rB, CuKα radiation, λ = 0.1542 nm, 40 kV, 100 mA) and Micro laser Raman spectroscope (HR800). Optical properties of the spindle-like ZnO microcrystals were also investigated by photoluminescence spectroscopy (PL SPEX FL-2T2).

* Corresponding authors. Fax: +86 451 88060653.
E-mail addresses: wuxiang05@gmail.com (X. Wu), mzan@hit.edu.cn (M. An).

0925-8388/$ – see front matter © 2010 Elsevier B.V. All rights reserved.
doi:10.1016/j.jallcom.2010.04.110

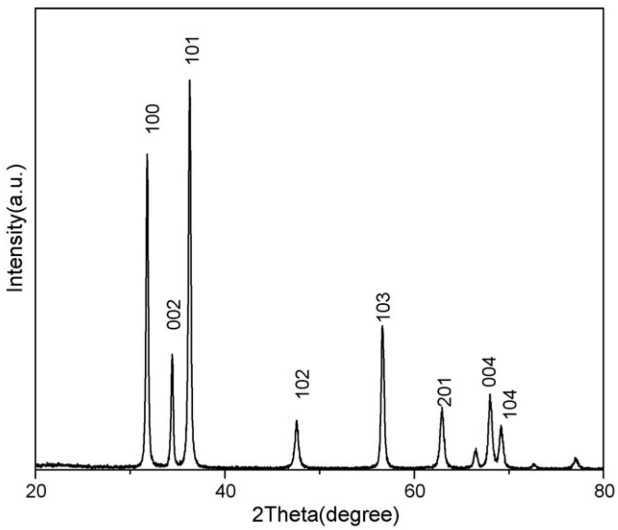

Fig. 1. XRD pattern of spindle-like ZnO microcrystals.

3. Results and discussion

Fig. 1 shows a representative XRD pattern of the as-prepared product. All diffraction peaks at 2θ degrees ranging from 25° to 80° can be indexed as hexagonal wurtzite ZnO structure comparable to the standard data (JCPDS cards file, No. 36-1451). No peaks from other structures are observed, indicating the high purity of the product.

Typical SEM images of the as-synthesized product are presented in Fig. 2(a and b). From these images, one can see that almost all of the produced ZnO structures have the representative spindle-like shape and the yield is very high. The ZnO spindle-like microcrystals have an average diameter of about 200 nm and lengths of about 1 μm according to these images.

TEM is utilized to characterize the microstructure of as-grown ZnO spindle-like microcrystals. Fig. 3(a) shows a low-magnification TEM image of a single ZnO microcrystal, from which the spindle-like shape with two tips located at two sides are clearly seen, in accordance with the SEM results. The spindles have diameters ranging from 220 nm in the center to 50 nm around the corner. A typical SEAD pattern taken from the spindle is showed in Fig. 3(a) inset, indicating that as-grown ZnO microcrystal is of single crystal structure and grows along the [0 0 0 1] direction. Fig. 3(b) shows a high-resolution TEM (HRTEM) image taken from the ZnO spindle. The clearly resolved lattice fringe is about 0.26 nm, in accordance with the (0 0 0 2) plane of wurtzite ZnO phase. The result also confirms the growth direction of the ZnO spindle is along the [0 0 0 1] orientation.

Fig. 4 is a representative Raman spectrum of the obtained product, where several Raman peaks can be clearly seen. Among these peaks, the strongest one was found located at about 440 cm^{-1}. According to selection rule of phonon mode [25], it can be attributed to non-polar optical phonon mode associated with oxygen deficiency. Besides the strongest Raman mode, the Raman spectra also show other modes with frequencies of 202, 333, 585 and 1155 cm^{-1}.

To study the growth mechanism of spindle-like ZnO microcrystals, controlled experiments with different experimental parameters were performed. Fig. 5 is the time-dependent SEM

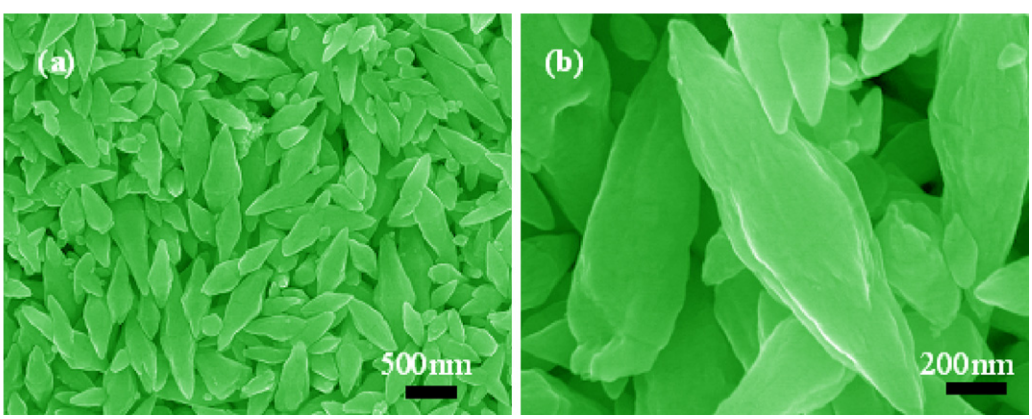

Fig. 2. Typical SEM image of spindle-like ZnO microcrystals (a) low-magnification image and (b) high magnification image.

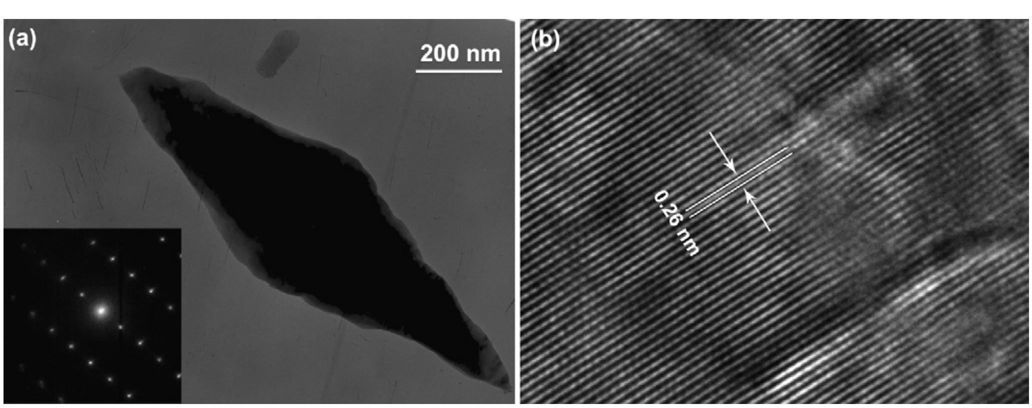

Fig. 3. TEM image of spindle-like ZnO microcrystals (a) low-magnification TEM image and the inset is the corresponding SAED pattern. (b) the HRTEM image.

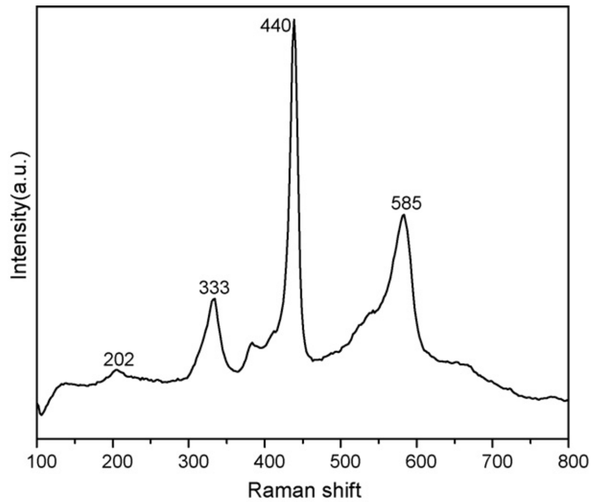

Fig. 4. Room-temperature Raman spectrum of spindle-like ZnO products.

images of the synthesized products, where the experiments were performed with different reaction time. Fig. 5(a and b) is SEM images of the product after 1 h, some flower-like structures consisted of short nanocones can be seen. When the reaction time was prolonged to 2 h, the sizes of the flower-like structure became large and the flowers consisted of spindles instead of nanocones compared with the product after 1 h, as shown in Fig. 5(c and d). Fig. 5(e) shows a SEM image of the ZnO products after 4 h, from which large quantities of individual spindles with average diameter of 200 nm can be seen. However, no individual spindles are formed when the reaction time is increased to 8 h (Fig. 5(f)). This means that the reaction time of 6 h is suitable to form spindle-like ZnO structures. The pH value of the solution also plays an important role to the final morphologies of as-synthesized products. Spindle-like ZnO microcrystals reported here are synthesized when the pH value is 10. When the pH value lowered to 8, large quantity of flower-like structures by assembly of nanocones can be found, and also some nanocrystals appeared, as shown in Fig. 6(a). However, when pH value reached 11, though there were some spindles existed, most of them were the case that two spindles connected cross instead of single one, just as indicated in Fig. 6(b).

In the previous reports, Wu and co-workers synthesized AlN nanocones through the reaction between $AlCl_3$ and NH_3 at 700 °C with Mo grid as a mask and investigated the FE performance of AlN nanocones [26]. Bae et al. reported ZnO nanocones through pulsed laser deposition [27]. High-density cubic BN nanocones have been fabricated from cubic BN/diamond composite films by bias-assisted reactive ion etching with the assistance of gold dot masks [28], ions of lower kinetic energy were thought to lead to the formation of cubic BN conical structure. Herein we successfully synthesized spindle-like ZnO microcrystals in an aqueous solution at low temperature without any surfactant or template. From the

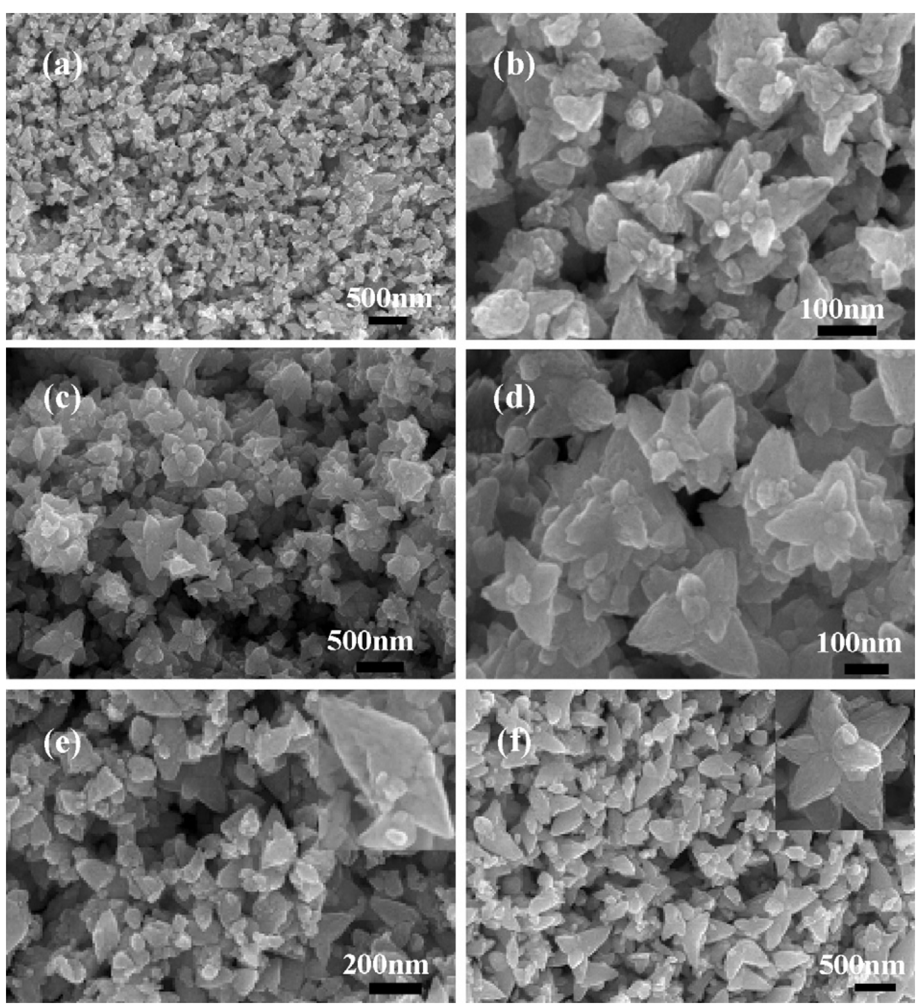

Fig. 5. Effect of reaction time on the morphologies of the ZnO products. (a and b) $t = 1$ h, (c and d) $t = 2$ h, (e) $t = 4$ h and (f) $t = 8$ h.

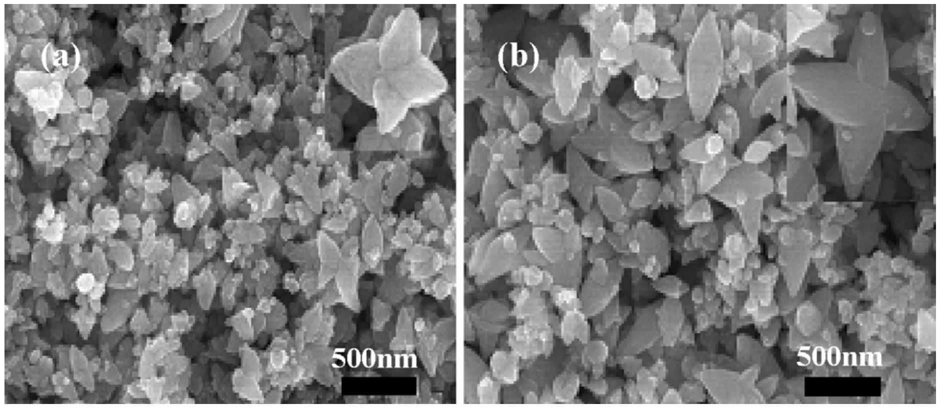

Fig. 6. Effect of pH value of solution on the morphologies of the products (a) pH 8 and (b) pH 11.

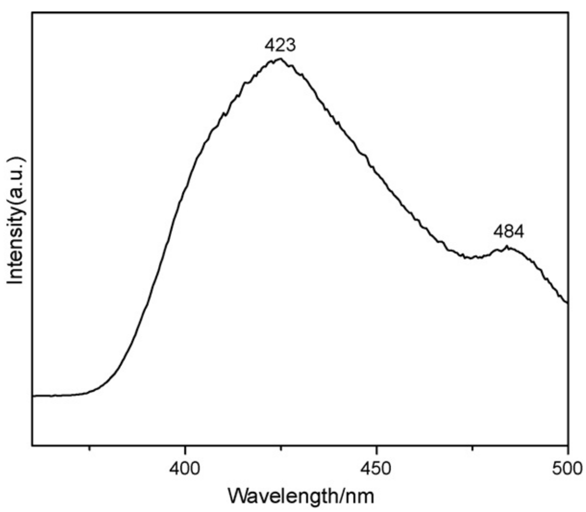

Fig. 7. Room-temperature PL spectra of spindle-like ZnO microcrystals.

crystallization point of view, the growth of the nanomaterial is a process of nucleation and growth. At earlier stage, $Zn(OH)_2$ formed through Zn^{2+} and OH^-. With reaction process, the nucleation and crystal growth rate would be higher. The $Zn(OH)_2$ and OH^- reacted with each other and created more ZnO^{2-} nuclei. Then these ZnO^{2-} nuclei interacted with water molecules and can be fused small ZnO particles due to the kinetic process of crystal growth. The resultant shape of as-obtained product was dominated by kinetics and thermodynamics. At the elevated temperature, ZnO small particles would spontaneously aggregate together under the function of the crystal polarity and concentration of alkali ion. The final shapes become more uniform and regular due to the continuous nucleation and growth. When the reaction proceeded to 11 h, the perfect ZnO spindles could be obtained. At the same time, the pH value of the solution may be the key factor to confine the formation of spindle-like ZnO microcrystals. The detailed growth mechanism needs further investigation and will be reported in later work.

Finally, the room-temperature PL properties of the product were also investigated. Fig. 7 depicts a photoluminescence (PL) spectrum of as-grown spindle-like ZnO microcrystals, where a strong visible emission band centered at 423 nm and a weak emission around 484 nm are clearly seen. Previously, the visible emissions from different ZnO nano/microcrystals were widely reported [29–31]. Recently, Zeng et al. systemically studied the origins of the visible luminescence, including the peaks at about 420 and 480 nm of ZnO nanoparticles, and suggested these blue luminescence bands are related to zinc interstitials [32]. Based on these results, we can deduce that the synthesized spindle-like ZnO microcrystals own high density of defects. The synthesized ZnO microcrystals presented here may be used in optical and optoelectronic fields.

4. Conclusions

In summary, we have successfully synthesized spindle-like ZnO microcrystals with an average diameter of about 200 nm by a simple solution method at low temperature. As-synthesized ZnO microcrystals are single crystals with a wurtzite structure and grow along the [0 0 0 1] direction. Studies demonstrated that these interesting ZnO microspindles have a strong UV emission peak at 423 nm and a poor peak at 484 nm, which means that they can be used as a candidate to fabricate optoelectronic nanodevices.

Acknowledgements

This work was supported by the Doctor Start-up Fund of Harbin Normal University (KGB200802), the National Natural Science Foundation of China (20871037), the Natural Science Foundation of Heilongjiang Province (B2007-2), the Science Technology and Research Project of Education Bureau, Heilongjiang Province (11531229, 12531236).

References

[1] X.S. Fang, Y. Bando, M.Y. Liao, U.K. Gautam, C.Y. Zhi, B. Dierre, B.D. Liu, T.Y. Zhai, T. Sekiguchi, Y. Koide, D. Golberg, Adv. Mater. 21 (2009) 2034.
[2] X.S. Fang, Y. Bando, G.Z. Shen, C.H. Ye, U.K. Gautam, P.M.F.J. Costa, C.Y. Zhi, C.C. Tang, D. Golberg, Adv. Mater. 19 (2007) 2593.
[3] X.H. Sun, W.T. Liu, D.X. Ouyang, J. Alloys Compd. 478 (2009) 38.
[4] J.H. He, C.L. Hsin, J. Liu, L.J. Chen, Z.L. Wang, Adv. Mater. 19 (2007) 781.
[5] S.J. Chang, T.J. Hsueh, C.L. Hsu, Y.R. Lin, I.C. Chen, B.R. Huang, Nanotechnology 19 (2008) 095505.
[6] D. Yeom, J. Kang, M. Lee, J. Jang, J. Yun, D.Y. Jeong, C. Yoon, J. Koo, S. Kim, Nanotechnology 19 (2008) 395204.
[7] K.D. Yuan, X. Yin, J.T. Li, J.J. Wu, Y.M. Wang, F.Q. Huang, J. Alloys Compd. 489 (2010) 694.
[8] Z.L. Wang, J.H. Song, Science 312 (2006) 242.
[9] Y. Shen, T. Yamazaki, Z. Liu, D. Meng, T. Kikuta, J. Alloys Compd. 488 (2009) L21.
[10] Y. Tao, M. Fu, A. Zhao, D. He, Y. Wang, J. Alloys Compd. 489 (2010) 99.
[11] H.B. Zeng, X.J. Xu, Y. Bando, U.K. Gautam, T.Y. Zhai, X.S. Fang, B.D. Liu, D. Golberg, Adv. Funct. Mater. 19 (2009) 3165.
[12] X. Wu, F. Qu, X. Zhang, W. Cai, G. Shen, J. Alloys Compd. 486 (2009) L13.
[13] Z.Y. Wang, Q.F. Lu, X.S. Fang, X.K. Tian, L.D. Zhang, Adv. Funct. Mater. 16 (2006) 661.
[14] G.Z. Shen, Y. Bando, C.Y. Zhi, X.L. Yuan, T. Sekiguchi, D. Golberg, Appl. Phys. Lett. 88 (2006) 243106.
[15] X. Wu, F.Y. Qu, G.Z. Shen, W. Cai, J. Alloys Compd. 482 (2009) L32.
[16] S. Jeong, E.S. Aydil, J. Cryst. Growth 311 (2009) 4188.
[17] J. Brown, F. Wu, P.M. Petroff, J.S. Speck, J. Cryst. Growth 84 (2004) 690.
[18] X. Wu, W. Cai, F.Y. Qu, Chin. Phys. B 18 (2009) 1669.
[19] X. Wu, P. Jiang, W. Cai, X.D. Bai, P. Gao, S.S. Xie, Adv. Eng. Mater. 10 (2008) 476.
[20] X. Wu, J.H. Sui, W. Cai, F.Y. Qu, Mater. Chem. Phys. 112 (2008) 325.
[21] J. Lee, M. Yoon, J. Phys. Chem. C 113 (2009) 11952.

[22] H.B. Chen, X. Wu, L.H. Gong, C. Ye, F.Y. Qu, G.Z. Shen, Nanoscale Res. Lett. 5 (2010) 570.
[23] G.Z. Shen, Y. Bando, D. Golberg, Int. J. Nanotechnol. 4 (2007) 730.
[24] X.R. Li, Y.Q. Wang, G.J. Song, Z. Peng, Y.M. Yu, X.L. She, J.J. Li, Nanoscale Res. Lett. 4 (2009) 10150.
[25] T.C. Damen, S.P.S. Porto, B. Tell, Phys. Rev. 32 (1966) 142.
[26] N. Liu, Q. Wu, C. He, H. Tao, X. Wang, W. Lei, Z. Hu, ACS Appl. Mater. Interfaces 1 (2009) 1927.
[27] J. Bae, J.I. Hong, W.H. Han, Y.J. Choi, R.L. Snyder, Chem. Phys. Lett. 475 (2009) 260.
[28] Y.S. Zou, Y.M. Chong, A.L. Ji, Y. Yang, Q. Ye, B. He, W.J. Zhang, I. Bello, S.T. Lee, Nanotechnology 20 (2009) 155305.
[29] G.Z. Shen, J.H. Cho, C.J. Lee, Chem. Phys. Lett. 401 (2005) 414.
[30] G.Z. Shen, Y. Bando, B. Liu, D. Golberg, C.J. Lee, Adv. Funct. Mater. 16 (2006) 410.
[31] G.Z. Shen, Y. Bando, D. Chen, B. Liu, C. Zhi, D. Golberg, J. Phys. Chem. B 110 (2006) 3973.
[32] H.B. Zeng, G.T. Duan, Y. Li, S.K. Yang, X.X. Xu, W.P. Cai, Adv. Funct. Mater. 20 (2010) 561.